JMEPEG (2015) 24:1834–1840
DOI: 10.1007/s11665-015-1449-6

1059-9495/$19.00

Investigation of the Oxidation Behavior of Orthorhombic Ti_2AlNb Alloy

Joanna Małecka

(Submitted November 7, 2014; in revised form February 17, 2015; published online February 28, 2015)

The results of investigation on the oxidation behavior of orthorhombic Ti_2AlNb alloy are presented. Oxidation was carried out in static air atmosphere at two temperatures: 700 and 800 °C. The investigation of the material structure of the specimen and chemical composition of oxidation products was performed. It was determined that the alloy shows a sufficient high-temperature corrosion resistance only at 700 °C.

Keywords corrosion and wear, oxidation, titanium

1. Introduction

In recent years, high-temperature titanium alloy development for aerospace applications has focused on γ-TiAl alloys. These alloys are a new type of materials and represent a very attractive structural material for operation at elevated temperatures and in aggressive chemical environments, mainly due to particularly favorable combination of mechanical properties and low density. Good creep resistance and relatively good oxidation resistance are their main assets which add to their versatile application (Ref 1–4). The research carried out so far by research centers have concerned the issue of high-temperature oxidation resistance of γ-TiAl-based alloys (Ref 5–11). Recent efforts to improve high-temperature properties have been directed toward the optimization of the Nb (Ref 12–14). However, the tendency to brittle fracture and low flow is their main shortcomings which limit their use. Recently, there has been a considerable interest in Nb-rich Ti_3Al alloys due to the discovery of an orthorhombic (O) phase based on the compound Ti_2AlNb (Ref 15). This orthorhombic phase was first found in a Ti-25Al-12.5Nb (at.%) alloy. The O phase is similar in nature to α_2 phase (Ti_3Al, DO19 structure), yet differs in the lattice arrangement of Nb with respect to Ti (Ref 15, 16). In Ti-alloy compositions ranging from 20 to 30 Al and 11 to 30 Nb the O phase has been identified (Ref 17, 18) and such alloys are often referred to as O alloys. Orthorhombic Ti_2AlNb-based alloys have outperformed α_2 alloys in terms of creep, tensile strength, ductility, toughness, and thermomechanical fatigue (Ref 19–22). These alloys appear to be quite promising for this application, but will find increased attention only if they offer a unique set of properties, not provided by competing alloys. For demanding applications in elevated temperatures, e.g., jet engines, this new class of alloys competes with conventional near-titanium alloys, the almost mature γ-TiAl alloys and, as all high-temperature titanium base alloys, with nickel-based materials (Ref 23).

Joanna Małecka, Faculty of Mechanical Engineering, Opole University of Technology, Opole, Poland. Contact e-mail: j.malecka@po.opole.pl.

In the Ti-Al-Nb system, the orthorhombic alloys based on Ti_2AlNb are generally constituted of some of the following phases: the α_2 phase (based on Ti_3Al, hexagonal DO19 structure), the O phase (based on Ti_2AlNb, orthorhombic distortion of the α_2 phase), and the β0 (or B2) phase (based on Ti_2AlNb, ordered from the bcc β-phase) (Ref 24).

For mechanical optimization several alloying elements are added, which show specific phase stabilization properties:

Mo—is reported to reduce the oxygen solubility and thus to inhibit internal oxidation (Ref 25).

Nb is a β-forming element so it causes the formation of β-Ti(Nb) phase in α_2 and γ phases. It reduces the solubility of the oxygen thus preventing internal oxidation of these alloys (Ref 26–28). Introducing niobium as an alloying additive makes niobium ions replace Ti—leading to reduction of vacancies in oxygen, which limits the diffusion of oxygen (Ref 29). Niobium improves the resistance to oxidation if it forms a solid solution with the scale. If, however, it occurs in the form of $TiNb_2O_7$ or $AlNbO_4$ phase, it decreases the oxidation resistance. The effect of niobium in Ti-Al also consists in hindering the mass transfer of TiO_2 (Ref 13).

V—promotes the improvement of the plasticity of alloys (Ref 30).

Relatively few works have been reported on the oxidation behavior of orthorhombic alloys (Ref 31–33). This work aims to shed light on the oxidation and scale formation mechanisms in orthorhombic Ti-Al-Nb alloys (Ti-22Al-25Nb alloy). In the present paper the isothermal oxidation behavior of orthorhombic alloy (Ti-25Al-12.5Nb) was studied in static air atmosphere for two temperatures: 700 and 800 °C.

2. Experimental Procedures

The tests were performed on O-Ti_2AlNb-based alloy Ti-25Al-12.5Nb (at.%) with the content of β-stabilizing elements: Mo (3.0 at.%) and V (0.48 at.%). Isothermal oxidation experiments were performed in static air atmosphere at the temperature 700 and 800 °C during 500 h. Oxidation tests were carried out on rectangular coupons of 20 × 15 × 2 mm. The samples were ground on abrasive paper of 800 grade paper and subsequently degreased in acetone.

The computer-aided acquisition system was used to verify the actual test temperature. After the test exposure, mass

changes due to oxidation processes were controlled by a precision scale with accuracy of 10^{-4} g. Trials were repeated three times and the presented test results were averaged.

After the test was finished, surfaces and cross section of the oxidized specimen were characterized. They were studied by scanning electron microscopy (SEM) and were also subjected to energy-dispersive x-ray microanalysis. Investigations of the material structure and chemical constitution in the micro-areas of the specimens were performed using a JEOL JSM-35 microscope equipped with a WDS analyser.

3. Results and Discussion

The microstructure of orthorhombic titanium aluminides may vary widely depending on processing methods and subsequent heat treatments (Ref 34). The classification of orthorhombic alloys allows distinguishing typical microstructures: (a) equiaxed, (b) bimodal, (c) lamellar, (d) lamellar with coarse secondary O laths and thick grain-boundary α_2 phase.

The structure of the tests alloy is presented in Fig. 1, and the type can be established as lamellar. It is a typical microstructure generated as a result of the recrystallization of the material.

3.1 Oxidation Behavior of the Alloy

The oxidation kinetics of the alloy is presented in Fig. 2. And thus the oxidation in air at 700 and 800 °C during 500 h caused the mass gain which intensifies at 800 °C.

For the purpose of verification, the oxidation tests were carried out three times using the same research methodology, which enabled a more precise analysis of the process' progress. It can be concluded that the tests are characterized by a high repeatability of results. The demonstration of repeatability is show in Fig. 2 (dashed curves).

The average mass gain and the standard deviation were as follows:

- at the temperature of 700 °C: 0.0464 mg/cm^2 after 50 h (standard deviation σ = 0.0247), 0.1694 mg/cm^2 after 100 h (standard deviation σ = 0.0448), 0.1795 mg/cm^2 after 300 h (standard deviation σ = 0.0164), and 0.1931 mg/cm^2 after 500 h (standard deviation σ = 0.0253).
- at the temperature of 800 °C: 0.4183 mg/cm^2 after 50 h (standard deviation σ = 0.0460), 0.5887 mg/cm^2 after 100 h (standard deviation σ = 0.0491), 0.8274 mg/cm^2 after 300 h (standard deviation σ = 0.0616), and 1.0881 mg/cm^2 after 500 h (standard deviation σ = 0.0215).

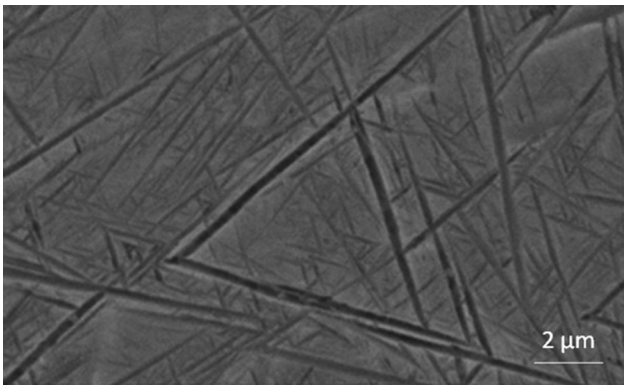

Fig. 1 Scanned images (SE) of Ti-25Al-12.5Nb alloy

At the temperature of 700 °C, the thermogravimetric curve was characterized by a big mass gain in the initial period lasting about 100 h, and subsequent noticeable slow-down. As can be seen after 500 h, the mass gain of the alloy is far smaller than that at 800 °C. Up to 500 h, the mass change did not exceed 0.2 mg/cm^2.

At the temperature of 800 °C, the thermogravimetric curve was characterized by an exceptionally big mass gain during the oxidation test. The mass change progressively increases, reaching about 1.1 mg/cm^2 after 500 h.

The scale forming on the surface of samples was tightly attached to the substrate and did not chip either immediately after the test or later. But, at 800 °C, the alloy shows approximately linear, not parabolic, oxidation kinetics. As observed at 800 °C the alloy shows normalized weight gain, but the kinetics were significantly different. After a first period of a protective behavior, alloy shows an approximately linear behavior after 100 h, and then after 300 h the oxidation rate accelerates. The oxide scales were brittle and showed local cracking after cooling, but there was no evidence of spallation during the experiments.

The growth rate of oxidation products strongly depends on the temperature, and the occurring diffusion processes are activated with the rise of the temperature and the oxidation time. It was noticed that at 700 °C the thickness of the forming scale determined the color of the Ti-25Al-12.5Nb alloy surface, which provides significant information.

Figure 3 shows the obtained coloring of the surface of Ti-25Al-12.5Nb alloy during the trials. The content of oxygen and nitrogen in the metallic substrate is the outcome of the atmosphere, the temperature, and the time of exposure to annealing. Along with the increase of temperature and time, the content of nitrogen and oxygen rises. Nitrogen is characterized by a high chemical affinity to titanium, higher than the oxygen. The formed nitrides are easily recognizable by the golden coloring of the surface. The mass gain resulting from bonding the oxygen and nitrogen and their resolving in the metallic substrate is rather moderate for this temperature. After 50 hours of isothermal heating in air, the surface of the alloy took a straw-yellow color (Fig. 3a). Doubling the oxidation time causes the alloy surface to take a purple shade (Fig. 3b) while the oxide layer growth during 300 h results in the blue surface with minor inclusions of purple (Fig. 3c). After 500 h of oxidation where the formed layer is thickest, the scale is of brown color (Fig. 3d). It is, however, worth noticing that such a

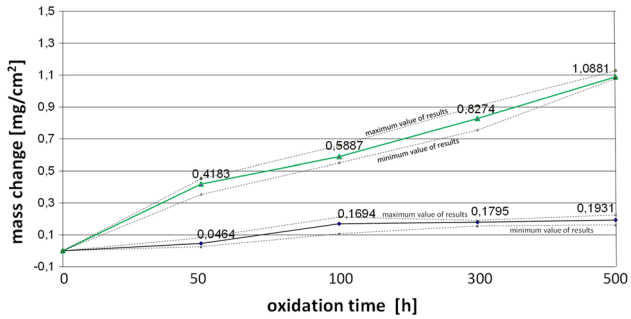

Fig. 2 The mass change of Ti-25Al-12.5Nb oxidized isothermally at 700 and 800 °C

coloring was obtained only in heating at 700 °C. The rise of the temperature up to 800 °C does not promote such a distinct coloring of the surface (Fig. 3e).

3.2 The Characteristics of the Forming Oxide Layers

The analyzed alloy is characterized by the formation of scale as the reaction product and the formation of the diffusion area of interstitial elements in the metallic substrate. Oxide layers forming during annealing consist of a few characteristic sublayers with similar structure and chemical composition.

The oxidized surface of substrate showed porous structure. According to XRD results, TiO_2 was the major phase and few Al_2O_3 phases appeared in the oxidated region the outer layer (I), which caused a loose, porous surface in morphology (Fig. 4).

At the temperature 700 °C, the surface characterized by quite an irregular structure in the form of particular eruptions (Fig. 5), loosely covering the sublayer. The oxidation of the alloy at 800 °C results in the formation of larger efflorescences (crystallite) on the surface (Fig. 6). Such a growth mode causes that voids of fractions of micrometers between outer layer and another sublayer close. The efflorescences, crystallite shaped, are identical with the ones observed by Król (Ref 35) on 'cp' titanium and identified as an allotropic form TiO_2-named rutile. The formation of columnar crystallites of rutile requires an explanation. These crystallites are positioned at different angles from each other and from the surface they grow out of. This product is formed not only as a result of the out-core diffusion of titanium ions, but also as a result of surface diffusion. Król (Ref 35) based the interpretation of such a growth on the model presented by Jungling and Rapp (Ref 36). The research of Rapp and associates (Ref 37–39) using HSESEM (Hot-Stage Environmental Scanning Electron Microscope) and video cameras for recording purposes proved that surface diffusion is the quickest process in a lower oxidation temperature, which leads to the formation of whiskers. A little participation of lattice diffusion causes their extension; that is the growth in the perpendicular direction. As the temperature increases, the participation of the lattice diffusion becomes significant which makes the growth of the oxide occur rapidly over the whole surface of grain, and in the dislocation area, stress and surface energy are reduced by the inward growth of the cavity. The observed crystallites are then formed with the co-influence of both types of diffusion. It confirms that an out-core transport of titanium ions occurs through the layer of products rich in Al_2O_3 as well as TiO_2. It also proves that a sublayer of Al_2O_3 homogeneous enough to prevent diffusion processes, thus increasing oxidation resistance, did not form.

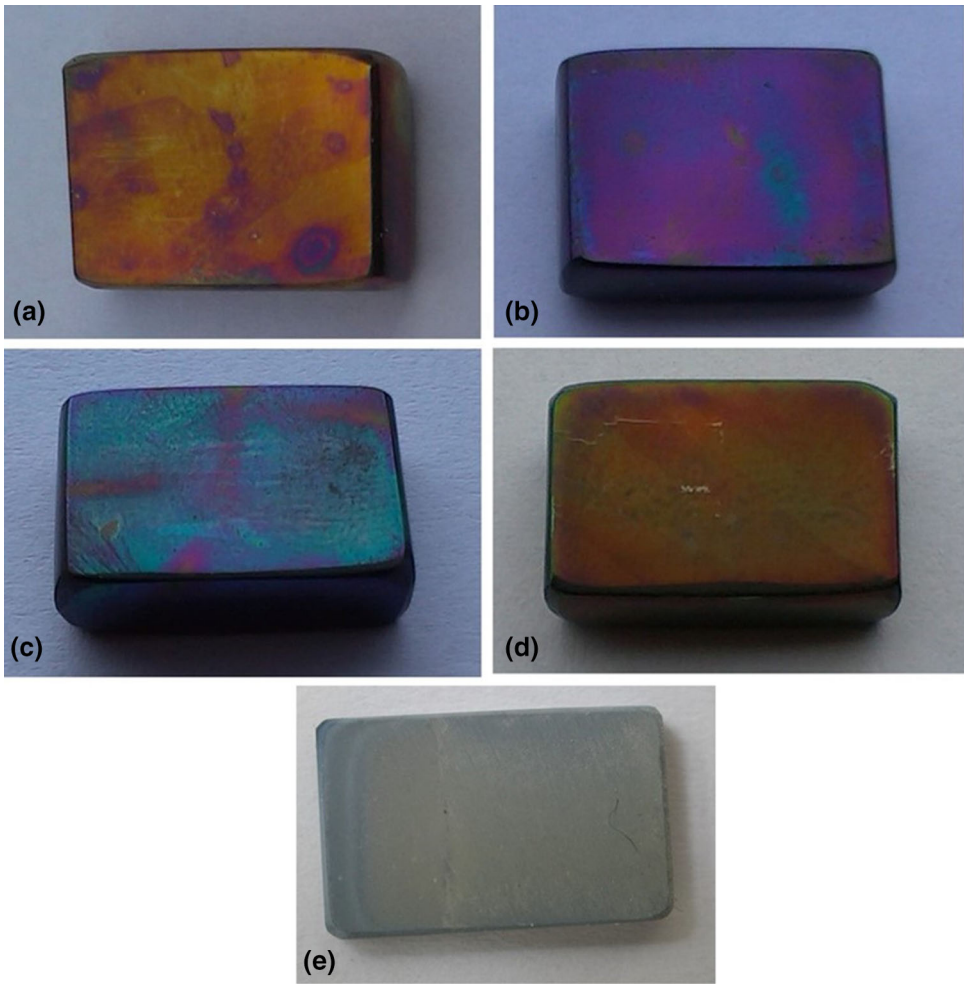

Fig. 3 Surface of Ti-25Al-12.5Nb alloy after isothermal oxidation at 700 °C after 50 h (a), 100 h (b), 300 h (c), 500 h (d) after isothermal oxidation at 800 °C (e)

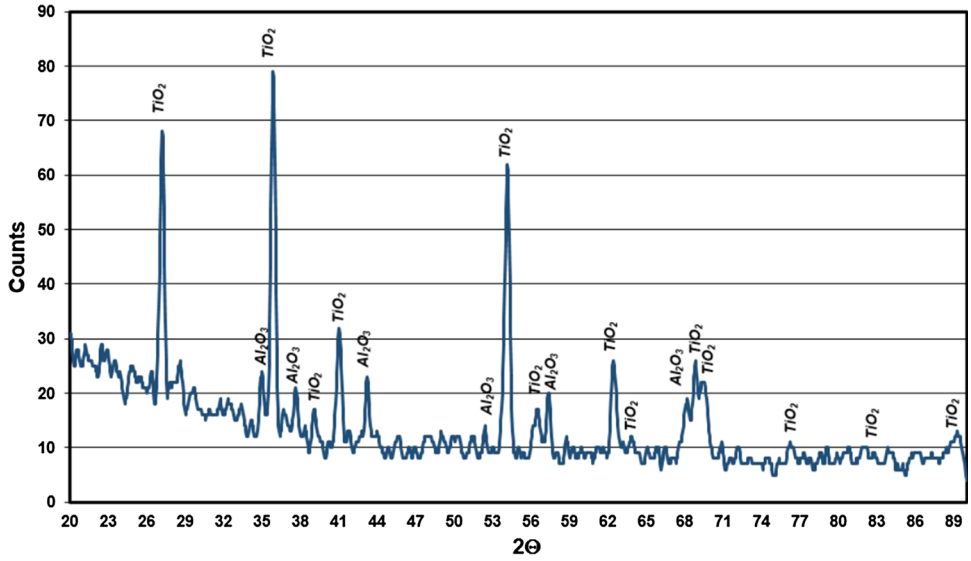

Fig. 4 XRD microanalysis result of surface specimen after oxidation in air

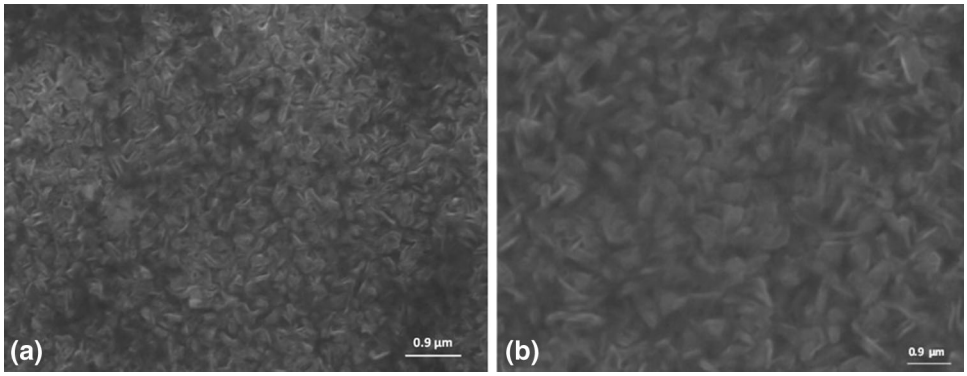

Fig. 5 The surface Ti-25Al-12.5Nb alloy after isothermal oxidation in air at 700 °C after 50 h (a) after 500 h (b)

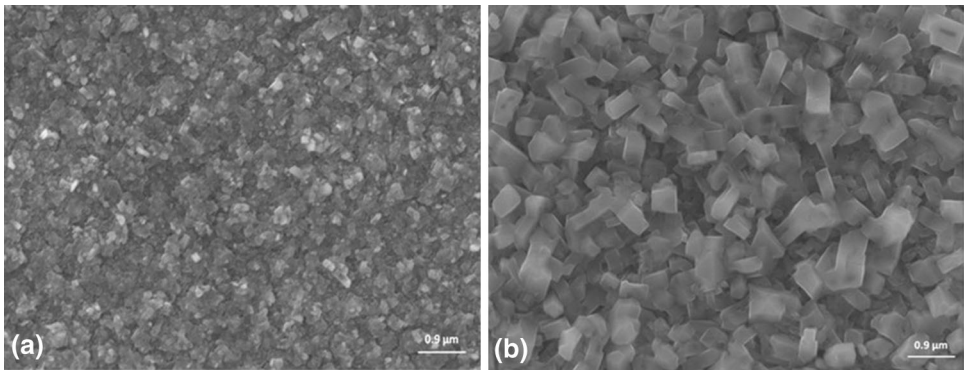

Fig. 6 The surface Ti-25Al-12.5Nb alloy after isothermal oxidation in air at 800 °C after 50 h (a) after 500 h (b)

The middle sublayer (II) forms a band running parallel to the oxidized surface and characterized by a graphite-gray contrast in BSE, which is, however, heterogeneous (Fig. 7, 8). Micro-analysis of this sublayer shows the dominance of Al with a much lower share of Ti (Tables 1 and 2). Probably, this band has a lot of Al_2O_3 but little TiO_2. Since these oxides occur separately, it results in the heterogeneity of the contrast and strong diversification of the composition in nano-areas.

Aluminum cations which diffuse out-core (slower than Ti) form Al_2O_3 with the oxygen. A protective layer will be formed from the reaction products only when they exclusively contain Al_2O_3. The formed layer of Al_2O_3 is heterogeneous and not

compact. Rutile TiO_2 is also present in its composition, however, in lower quantities. The presence of even a little quantity of TiO_2 in the sublayer rich in Al_2O_3 allows bidirectional diffusion and, as a result, the growth of the product on the outer surface as well as on the product-metallic substrate interface.

The inner layer (III) contains comparable volumes of Al_2O_3 and TiO_2, and locally higher quantities of TiO_2. Moreover, it contains oxides of alloying elements included in the composition of the analyzed alloy. Catenary microbands can be distinguished in this sublayer enriched in niobium, arranged parallel to the surface of the oxidized specimen.

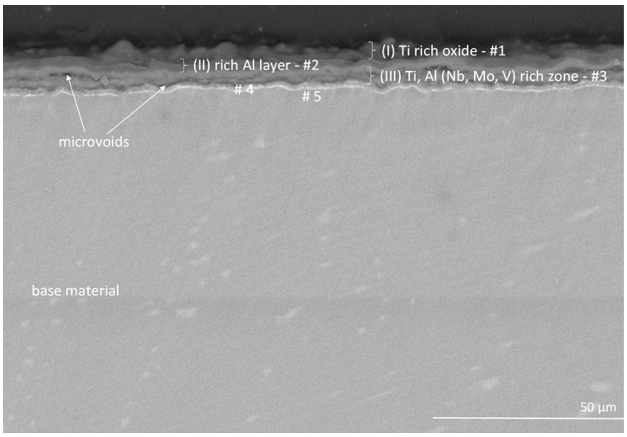

Fig. 7 Cross section of products and metallic sublayer of the oxidized Ti-25Al-12.5Nb alloy after 500 h at 700 °C (BSE image)

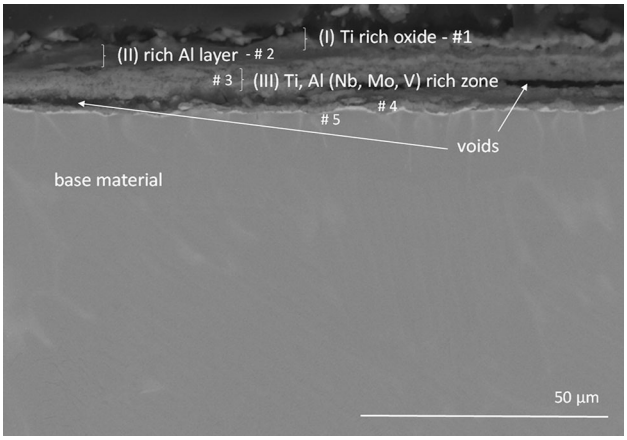

Fig. 8 Cross section of products and metallic sublayer of the oxidized Ti-25Al-12.5Nb alloy after 500 h at 800 °C (BSE image)

As it was determined, however, the remaining alloying elements add to changing the mass transfer course through the product layer. The performed test proved that the analyzed alloy also included elements from the metallic substrate. Therefore Nb, Mn, and V co-form oxides in each sublayer, so they diffuse quite rapidly and cannot cause the improvement of oxidation. However, the presence of Nb in the oxide sublayers below the columnar rutile sublayer suggests that its ions diffuse more slowly than Ti.

Microvoids occur between this sublayer and the metallic substrate. As the temperature rises the number of microvoids rises, as well as their size and their tendency to join is observed (Fig. 7, 8). The structure of this phase boundary determines the possibility of scale buckling during cooling.

3.3 The Diffusion of Oxygen, Nitrogen, and Alloying Elements in the Alloy and Products

The diffusion in a product of oxidation is bidirectional due to its phase composition in the layer cross section. Ions of alloying elements included in the composition of the analyzed alloys diffuse out-core. In the oxidation temperature closer to 800 °C, a small part of titanium ions also diffuse out-core, building columnar rutile crystallites over the (middle) sublayer rich in Al_2O_3. By diffusing out-core, aluminum forms Al_2O_3 near the surface. Since titanium simultaneously diffuses out-core, a two-phase Al_2O_3 + TiO_2 layer is formed instead of a one-phase layer of Al_2O_3. The presence of TiO_2 through the whole cross section secures a continuous flux of titanium ions migrating toward the surface. The degree of defecting in the cationic sublattice increases with the temperature rise so the quantity of Ti^{+3} and Ti^{+4} diffusing out-core goes up. The presence of TiO_2 through the whole cross section of the product layer creates favorable conditions for the in-core diffusion of oxygen and nitrogen due to the existence of oxygen vacancies. Therefore, the layer growth also occurs at the product-surface interface.

Oxidation does not only comprise diffusion processes discussed but also transformations occurring in the substrate at the interface between the substrate and scale. These transformations are caused by the "migration" of alloy-forming elements and formation of phases and solid solutions resulting from the in-core diffusion of N and O. The nitrogen diffusing through the layer does not form nitrides but, migrating toward the metallic substrate, forms Ti_2AlN or Ti_3AlN most probably. Therefore, the nitrogen absent in the cross section of the oxidized layer is concentrated in large quantities at the interface between the product and the metallic substrate. A distinctive area was observed there that was situated parallel to the oxidized surface (marked as #4 in picture 7-8). In this research, up to a dozen percent of nitrogen and oxygen was found in the region adjacent to the product interface (Tables 1 and 2).

Table 1 WDS-analysis (at.%) of locations labeled on Fig. 7

Location	N	O	Al	Nb	Ti	Mo	V
#1	0.00	54.40	12.46	5.35	27.79	…	…
#2	0.00	53.95	31.24	0.36	13.27	0.61	0.47
#3	0.00	51.58	19.72	2.37	25.48	0.85	…
#4	14.24	18.46	18.73	10.93	35.47	1.81	0.36
#5	3.70	7.63	25.27	11.07	48.94	2.97	0.42

Table 2 WDS-analysis (at.%) of locations labeled on Fig. 8

Location	N	O	Al	Nb	Ti	Mo	V
#1	0.00	59.49	11.84	4.85	23.82	…	…
#2	0.00	55.62	37.27	0.72	5.83	0.56	
#3	0.00	54.98	21.00	1.98	20.87	0.80	0.37
#4	16.60	19.00	20.82	8.91	33.35	1.20	0.12
#5	2.44	11.79	26.96	10.98	44.44	3.01	0.38

Orthorhombic alloys are particularly sensitive to embrittlement due to surrounding's impact. Oxygen and nitrogen, occurring in the transitory region between the scale and the substrate, promote embrittlement of the subsurface layer caused by the formation of nitride layer and the penetration by oxygen/nitrogen (voids observed in Fig. 7, 8). The addition of niobium in the analyzed alloy contributes to decreasing the rate of oxidation as it stabilizes O phase. The solubility of oxygen and nitrogen in O-Ti_2AlNb phase is definitely higher than within phase β of the allotropic variation of titanium. Niobium is in turn a β-forming element with respect to titanium so it promotes the formation of β-Ti(Nb) phase with a lower solubility of nitrogen and oxygen and driving to stabilize nitrides in this region which results in decreasing the oxidation rate.

4. Conclusions

This paper describes the kinetics of oxidation and the oxide scale morphologies on Ti_2AlNb orthorhombic alloy for isothermal oxidation at 700 and 800 °C in static air.

A multiphase scale forms during the oxidation of the Ti-25Al-12.5Nb alloy. The scale is characterized by an identical sequence of sublayers: an outer layer with a structure made of a mixture of TiO_2 and a smaller quantity of Al_2O_3, a heterogeneous inter-layer dominated by Al_2O_3 and with a low quantity of TiO_2, and the inner layer with comparable quantities of TiO_2 and Al_2O_3. In respective sublayers, there are also oxides of Nb, Cr, Ni.

Acknowledgment

The research study was financed from the funds for science in 2013-2015 as research project no. IP 2012 055772.

References

1. H. Clemens and H. Kestler, Processing and Applications of Intermetallic γ-TiAl-Based Alloy, *Adv. Eng. Mater.*, 2000, **9**, p 551–570
2. M. Yoshihara and Y.W. Kim, Oxidation Behaviour of Gamma Alloys Designed for High Temperature Oxidation, *Intermetallics*, 2005, **13**, p 952–958
3. M. Yamaguchi, H. Inui, and K. Ito, High-Temperature Structural Intermetallics, *Acta Mater.*, 2000, **48**, p 307–322
4. S. Danaher, T. Dudziak, P.K. Datta, R. Hasan, and P.S. Leung, Long-Term Oxidation of Newly Developed HIPIMS and PVD Coatings with Neural Network Prediction Modelling, *Corros. Sci.*, 2013, **69**, p 322–337
5. P. Schaaf, W.J. Quadakkers, N. Zheng, E. Wallura, and A. Gil, Beneficial and Detrimental Effects of Nitrogen on the Oxidation Behaviour of TiAl-Based Intermetallics, *Mater. Corros.*, 1997, **1**, p 28–34
6. N. Toshio, I. Takeshi, M. Yatagai, and T. Yoshioka, Sulfidation Processing and Cr Addition to Improve Oxidation Resistance of TiAl Intermetallics in Air at 1173 K, *Intermetallics*, 2000, **8**, p 371–379
7. V. Shemet, A.K. Tyagi, J.S. Becker, P. Lersch, L. Singheiser, and W.J. Quadakkers, The Formation of Protective Alumina-Based Scales During High-Temperature Air Oxidation of γ-TiAl Alloys, *Oxid. Met.*, 2000, **54**, p 211–235
8. Y. Shen, X. Ding, and F. Wang, High Temperature Oxidation Behaviour of Ti-Al-Nb Ternary Alloys, *J. Mater. Sci.*, 2004, **39**, p 6583–6589
9. S.Y. Chang, The Isothermal and Cyclic Oxidation Behavior of a Titanium Aluminide Alloy at Elevated Temperature, *J. Mater. Eng. Perform.*, 2007, **16**, p 508–514
10. J. Małecka, W. Grzesik, and A. Hernas, An Investigation on Oxidation Wear Mechanisms of Ti-46Al-7Nb-0.7Cr-0.1Si-0.2Ni, *Corros. Sci.*, 2010, **52**, p 263–272
11. E. Godlewska, M. Mitoraj, and K. Leszczynska, Hot Corrosion of Ti–46Al–8Ta (at.%) Intermetallic Alloy, *Corros. Sci.*, 2014, **78**, p 63–70
12. V. Shmet, M. Yurechko, A.K. Tyagi, W.J. Quadakkers, and L. Singheiser, The Influence of Nb and Zr Additions on the High Temperature Oxidation Mechanism of γ-TiAl Alloys in Ar/O_2, *Gamma Titanium Aluminides 1999*, Y.-W. Kim, D.M. Dimiduk, and M.H. Loretto, Ed., The Minerals, Metals & Materials Society, Warrendale, 1999, p 783–790
13. H. Jiang, M. Hirohasi, Y. Lu, and H. Imanari, Effect of Nb on the High Temperature Oxidation of Ti-(0-50at.%)Al, *Scr. Mater.*, 2002, **46**, p 639–643
14. S. Król, J. Małecka, L. Zemčik, The Effect of Niobium on the Kinetics Oxidation Behaviour of γ-TiAl. Protection Against Corrosion 11s/A (2007) 124-128 (in Polish)
15. D. Banerjee, A.K. Gogia, T.K. Nandy, and V.A. Joshi, A New Ordered Orthorhombic Phase in a Ti_3Al_2Nb Alloy, *Acta Metall.*, 1988, **A36**, p 871–882
16. B. Mozer, L.A. Bendersky, and W.J. Boettinger, Neutron Powder Diffraction Study of the Orthorhombic Ti_2AlNb Phase, *Scr. Metall. Mater.*, 1990, **24**, p 2363–2368
17. K. Muraleedharan, A.K. Gogia, T.K. Nandy, D. Banerjee, and S. Lele, Transformations in a Ti-24Al-15Nb Alloy: Part I. Phase Equilibria and Microstructure, *Metall. Mater. Trans. A.*, 1992, **23A**, p 401–415
18. R.G. Rowe, D. Banerjee, K. Muraleedharan, M. Larsen, E.L. Hall, D.G. Konitzer, and A.P. Woodfield: in Titanium '92 Science and Technology, F.H. Froes and I. Caplan (Eds.) TMS, Warrendale, PA (1993) 1259-1266
19. J. Kumpfert, Intermetallic Alloys Based on Orthorhombic Titanium Aluminide, *Adv. Eng. Mater.*, 2001, **3**, p 851–864
20. D. Banerjee: Intermetallic Compounds Principles and Practice, J.H. Westbrook and R.L. Fleischer (Eds.) Wiley, New York, 2 (1994) 91–131
21. P.R. Smith, W.J. Porter, W.J. Kralik, and J.A. Graves: Metal Matrix Composites, Proc. 10th Int. Conf. on Composite Materials, Vol 2, A. Poursartip and K.N. Street, eds., Woodhead Publishing Ltd., Vancouver, BC, 1995, 731-738
22. P.R. Smith, J.A. Graves, C.G. Rhodes, M.R. James, and J.R. Porter, *Titanium Matrix Composites, WL-TR-92-4035*, OH, Wright-Patterson Air Force Base, 1992, p 115–145

23. J. Kumpfert and C. Leyens, Orthorhombic Titanium Aluminides, Intermetallics with Improved Damage Tolerance, *Titanium and Titanium Alloys, Fundamentals and Applications*, C. Leyens and M. Peters, Ed., WILEY-VCH Verlag GmbH & Co. KGaA, Weinheim, 2003,
24. K. Muraleedharan, T.K. Nandy, D. Banerjee, and S. Lele, Phase Stability and Ordering Behaviour of the O Phase in Ti-Al-Nb Alloys, *Intermetallics*, 1995, **3**, p 187–199
25. Y. Shida and H. Anada, Role of W, Mo, Nb and Si on Oxidation of TiAl in Air at High Temperature, *Metall. Mater. Trans. A*, 1994, **35**, p 623–631
26. S. Taniguchi and T. Shibata, T, Influence of Additional Elements on the Oxidation Behaviour of TiAl, *Intermetallics*, 1996, **4**, p 85–93
27. V.A.C. Haanappel, H. Clemens, and M.F. Stroosnijder, The High Temperature Oxidation Behaviour of High and Low Alloyed TiAl-Based Intermetallics, *Intermetallics*, 2002, **10**, p 293–305
28. J.W. Fergus, Review of the Effect of Alloy Composition on the Growth Rates of Scales Formed During Oxidation of Gamma Titanium Aluminide Alloys, *Mater. Sci. Eng. A*, 2002, **338**, p 108–125
29. T.K. Roy, R. Balasubramaniam, and A. Ghosh, High Temperature Oxidation of Ti3Al-Based Titanium Aluminides in Oxygen, *Metall. Mater. Trans. A*, 1996, **27**, p 3993–4002
30. T.T. Cheng, M.R. Wills, and I.P. Jones, Effects of Major Alloying Additions on the Microstructure and Mechanical Properties of γ-TiAl, *Intermetallics*, 1999, **7**, p 89–99
31. A. Ralison, F. Dettenwanger, and M. Schutze, Oxidation of Orthorhombic Ti2AlNb Alloys at 800 C in Air, *Mater. Corros.*, 2000, **51**, p 317–328
32. A. Ralison, F. Dettenwanger, and M. Schütze, Oxidation of Orthorhombic Ti2AlNb Alloys in the Temperature Range 550–1000 °C in Air, *Mater. High Temp.*, 2003, **20**, p 607–629
33. Ch Leyens, Environmental Effects on Orthorhombic Alloy Ti-22Al-25Nb in Air Between 650 and 1000 °C, *Oxid. Met.*, 1999, **52**, p 475–503
34. J. Kumpfert, H. Assler, D.B. Miracle, and J.E. Spowart, Transverse Properties of Titanium Matrix Composites, *Materials Week 2000*, Munich
35. S. Król, Mechanism and Oxidation Kinetics of Titanium and Selected Titanium Alloys (1994) Opole (in Polish)
36. T. Jungling and R.A. Rapp, High Temperature Oxidation of Iron at 1200 & #xB0;C in Hot-Stage Environmental Scanning Electron Microscope, *Metall. Mater. Trans A*, 1982, **134**, p 929–935
37. L. Matson, H. Erhart, M. Lee, and R.A. Rapp, Crystallographic and Morphological Characteristics of Oxidation Growth Pits in Wustite Grown at 1200 °C, *Metall. Trans.*, 1984, **15A**, p 2241–2246
38. G.M. Reynaud, W.A.T. Clark, and R.A. Rapp, In Situ Observation of Copper Oxidation at High Temperatures, *Metall. Trans.*, 1984, **15A**, p 573–586
39. R.A. Rapp, The High Temperature Oxidation of Metals Forming Cation Diffusing Scales, *Metall. Trans.*, 1984, **15A**, p 765–782